BUTTERWORTH HEINEMANN

Polymer Vol. 36 No. 15, pp. 2883–2894, 1995

0032-3861/95/$10.00 + 0.00

Cure kinetics and morphology of amine-cured tetraglycidyl-4,4′-diaminodiphenylmethane epoxy blends with poly(ether imide)

Chean C. Su and Eamor M. Woo*
Department of Chemical Engineering, National Cheng Kung University, Tainan, Taiwan 701-01, Republic of China
(Received 13 August 1994)

The cure kinetics and mechanisms of a diaminodiphenylsulfone-cured tetraglycidyl-4,4′-diaminodiphenylmethane epoxy and its blends with poly(ether imide) (PEI) of various compositions were studied using differential scanning calorimetry (d.s.c.). An autocatalytic mechanism was observed for the epoxy–PEI blends; however, the reaction rates for the epoxy blends were found to be higher than that of the neat epoxy. To understand the interrelationship between the cure kinetics and the morphological structure of the epoxy blends, the morphology evolution as a function of extent of cure was examined using scanning electron microscopy (SEM). The higher reaction rate observed in the epoxy blends is proposed to be caused by enhanced molecular mobility as a result of plasticization of the crosslinking epoxy networks by the PEI. In addition, phase separation of the epoxy–PEI blends during cure induced an uneven segregation of the epoxy and amine in different domains. These factors which affected the cure kinetics were discussed. The proposed kinetic model has been found to describe well the cure behaviour of the epoxy–PEI blends up to the vitrification point.

(Keywords: epoxy–poly(ether imide) blends; cure kinetics; morphology)

INTRODUCTION

Thermosetting epoxies possess many desirable properties such as high tensile strength and modulus, excellent chemical and solvent resistance, dimensional and thermal stability, good creep resistance, and excellent fatigue properties. These characteristics make them ideal candidates as matrices for many important applications including adhesives, electronics encapsulants, and matrix resins for high-performance fibre-reinforced composites. However, the epoxy resins are generally brittle due to high crosslink densities. Toughening epoxy matrices using liquid reactive rubbers has been widely reported in the literature[1–3]. However, the rubber modification of epoxies becomes ineffective as the crosslink density of the epoxy matrix increases due to the inability of the rubber particles to undergo shear yielding or cavitation when surrounded by a highly crosslinked network. Furthermore, toughness improvements in most rubber-modified thermosetting systems usually result in a significant decrease in the glass transition temperature (T_g) of the cured thermosetting resins. The T_g depression of the modified epoxy matrices can become severe, especially when the reactive rubbers are used at levels which are high enough to noticeably enhance the fracture toughness. As a result, alternatives were needed and recent studies have demonstrated that polymeric thermoplastics, such as poly(ether sulfone)s (PESs)[4,5], poly(ether imide)s (PEIs)[6,7], polycarbonate[8–10], and poly(phenylene oxide)[11], or a combination of rubbers and thermoplastics[12] etc., can enhance fracture toughness without sacrificing the T_g, strength, stiffness, or other desirable properties of thermosetting resin systems. Alloying with polysulfone or poly(ether sulfone) with reactive functional groups has also been the recent focus of toughness improvement for epoxy resins[13].

Attention has been focused on derivation of the reaction mechanisms of tetrafunctional epoxides with amines[14–17], and both empirical and mechanistic kinetic models have been derived. Since a completely rigorous approach is very difficult considering the complexity of the chemistry of the epoxy curing process, studies of epoxy–amine reactions using model compounds have also been attempted[18,19]. Although epoxy–amine reactions are rather complicated, depending on the reaction conditions, it is generally accepted that there are two important addition reactions, namely primary and secondary amine addition, as follows:

$$-\mathrm{R}-\underset{\diagdown\ \diagup}{\overset{\mathrm{O}}{\mathrm{CH}}}-\mathrm{CH_2} + -\mathrm{R'NH_2} \quad \text{(primary amine)}$$

$$\xrightarrow{k_1'} -\mathrm{R}-\mathrm{CH(OH)CH_2NH}-\mathrm{R'}- \qquad (1)$$

* To whom correspondence should be addressed

$$-R-CH-CH_2 + -R-CH(OH)CH_2NH-R' \quad \text{(secondary amine)}$$
$$\xrightarrow{k_2'} -R-CH(OH)CH_2N-R'-CH_2CH(OH)R'- \quad (2)$$

The third type of reaction that occurs to a certain extent at a later stage is etherification[20], which is a reaction between an epoxide and the OH group of the intermediate products from the previous two amine additions, as follows:

$$-R-CH-CH_2 + -R-CH(OH)CH_2NH-R'-$$
$$\xrightarrow{k_e'} -R-CHCH_2NH-R'-$$
$$\quad O-CH_2CH(OH)-R- \quad (3)$$

Etherification can occur intermolecularly to form crosslinks or intramolecularly to form cyclic rings (cyclization). Intramolecular etherification is expected to be faster than the intermolecular process since cyclization is less restricted by the molecular mobility of the reacting species. The reactivities of the above three types of reaction are not all the same. For example, the secondary amine addition is generally less reactive than the primary amine process, and the ratio k_2'/k_1' has been reported to be 0.5 or less, depending on the structural hindrance effect of the amines[20–23] or the presence of solvents[24]. The etherification occurs at the later stage, which might be retarded by the gelling network. As a result, the reaction kinetics determine the structure of the epoxy network that forms. On the other hand, a change in the structure of the epoxy network by, for example, addition of other polymers might also influence the reaction kinetics.

Thermoplastics addition to epoxy resins is thus expected to not only alter the morphology but also the cure kinetics. Phase separation takes place and a heterogeneous morphology develops if the thermoplastic polymer and the crosslinked epoxy are not miscible after cure. While the cure kinetics and reaction mechanisms of various neat epoxy resins have been extensively studied by the use of various methods, including i.r. spectroscopy[25,26] and more often, by differential scanning calorimetry[27–37], the effects of thermoplastic additives in epoxy resins on the cure kinetics have, however, rarely been investigated. In addition, phase morphology development during cure progress is also expected to significantly influence the properties of cured epoxy blends. In order to understand the reactivity characteristics and to predict the cure behaviour accurately for modified epoxy alloy systems, the objective of this study was to provide such critical information. By use of a kinetic modelling approach, we will show how thermosetting epoxy blends with a thermoplastic polymer (poly(ether imide)) will behave during cure. Correlation of the cure kinetics with morphology development of the heterogeneous epoxy system during cure progress was also examined.

EXPERIMENTAL

Materials

The epoxy resin used in this work is tetraglycidyl-4,4′-diaminodiphenylmethane (TGDDM) (Ciba–Geigy MY 720). It has a viscosity of 14 000 CP at 25°C as measured by a Haake viscometer. The base epoxy resin and its blends with the poly(ether imide) (PEI) (GE Ultem®-1010) were cured with an aromatic amine hardener, diaminodiphenylsulfone (DDS) (Ciba–Geigy HT976). The chemical structures of TGDDM, DDS, and PEI are as follows:

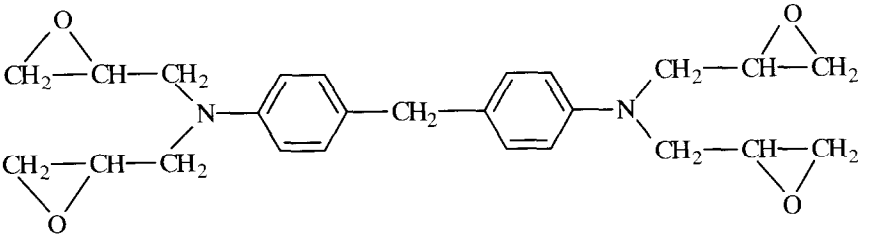

TGDDM

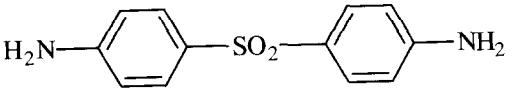

DDS

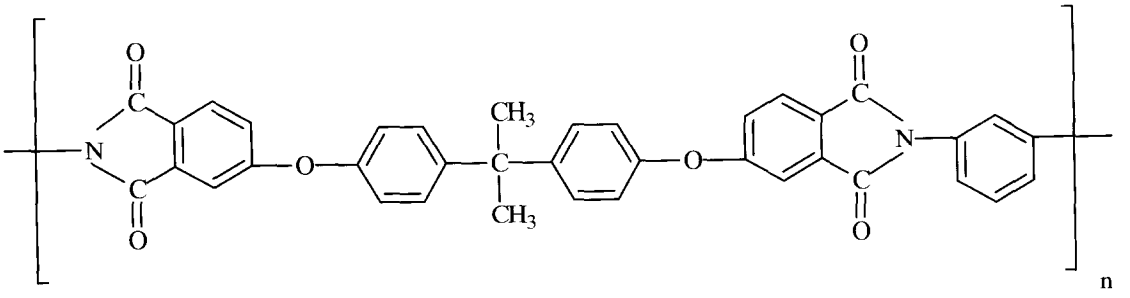

PEI

Epoxy/PEI blended resin mixtures with 10, 20, 30, and 50 phr of PEI, were prepared (where phr represents the number of parts of PEI per hundred parts of the TGDDM epoxy resin). First, PEI was weighed and dissolved completely in methylene chloride and the resulting polymer solution was then mixed with the epoxy resin at room temperature. The solvent in the mixture was vaporized in a circulation oven with an exhaust fan at room temperature, followed by removal of the residual solvent in a hot vacuum oven for 8 h at 120°C. Subsequently, 35 phr of DDS (= 0.67 stoichiometric equivalent of epoxy) was slowly added, with continuous stirring, to the resin–PEI mixture in an oil bath at 120°C.

To investigate the morphology change as a function of the progress of the reaction, a series of blend samples of various extents of cure were prepared. The polymer–epoxy blend samples were prepared in the oven at temperatures of 177, 187, and 197°C, and then withdrawn at different time intervals and quenched immediately to room temperature to 'freeze' the reaction. The epoxy blend samples in the various cure states were fractured and then sputter-coated for electron microscopy examination. To determine the extent of the epoxy reaction at the time of withdrawal from the oven, the residual isothermal heat for the samples was measured using d.s.c. The extent of reaction for the various samples was calculated from the relationship $\alpha_I = (\Delta H_{Io} - \Delta H_{IR}/\Delta H_T)$, where α_I is the extent of reaction, ΔH_{Io} is the total heat of reaction at 177°C, ΔH_{IR} is the residual heat of reaction, and $\Delta H_T = \Delta H_{Io} + \Delta H_R$.

Differential scanning calorimetry

A power-compensated type of differential scanning calorimeter (Perkin–Elmer DSC 7, equipped with an intracooler and a DEC computer for data acquisition/analysis) was used for the isothermal cure experiments and data analysis. Prior to the d.s.c. runs, the temperature and heats of reaction were calibrated using indium and zinc standards. Samples (5–8 mg) were placed in d.s.c. aluminium pans; since a clamped pan might be distorted due to thermal expansion of the sample, thus causing a severe shift of the d.s.c. baseline, special precautions had to be taken to ensure the stability of the baselines. A lid was placed on the sample pan without clamping to prevent ballooning due to thermal expansion of the sample at high temperatures. The instrument was capable of reaching the designated isothermal temperature at the fastest heating rate (500°C min^{-1}) and then equilibrating to the target temperature quickly. Thus, the heat of reaction that was lost (and thus not recorded) during the transient ramping was virtually negligible, which ensured the accuracy of the kinetic analysis.

Isothermal cure reaction was conducted at three temperatures (177, 187, and 197°C). The reaction was considered complete when the isothermal d.s.c. thermogram levelled off to the baseline, which generally took ~2 h. The total area under the exotherm curve, which was based on the extrapolated baseline at the end of the reaction, was used to calculate the isothermal heat of cure, ΔH_{Io} (J g^{-1}). After the cure reaction was completed in the calorimeter, the sample was cooled to 40°C. To determine the residual heat of reaction, ΔH_R (J g^{-1}), the samples after curing were scanned at 10°C min^{-1} from 40 to 300°C. The sum of both the isothermal heat (ΔH_{Io}) and residual heat (ΔH_R) of the reactions was taken to represent the total heat of cure (ΔH_T). The isothermal conversion at time t was defined as $\alpha_I(t) = \Delta H_I(t)/\Delta H_T$.

Electron microscopy

The morphology of the cured resins, as well as blends with various extents of cure was examined using a scanning electron microscope (JEOL, with two models, i.e. JSM-35 or JXA-840, being used). The fractured samples were coated with gold by vapour deposition using a vacuum sputterer. Some of the fractured samples were etched with solvent (methylene chloride) before they were sputter-coated and examined by microscopy.

Kinetic analysis procedures

A general equation for the autocatalytic cure reactions of many amine-cured epoxy systems is as follows[31–36]:

$$r = d\alpha/dt = (k_1 + k_2\alpha^m)(1 - \alpha)^n \quad (4)$$

where α is the conversion, k_1 and k_2 are the apparent rate constants, r is the rate of reaction, and m and n are the kinetic exponents of the reactions. The constant k_1 of equation (4) can be calculated if the initial reaction rate at $\alpha = 0$ can be estimated. Both kinetic constants, k_1 and k_2 are assumed to be of the Arrhenius form, i.e. $k_1 = A_1 \exp(-E_{a1}/RT)$ and $k_2 = A_2 \exp(-E_{a2}/RT)$, where A is the pre-exponential constant, E_a is the activation energy, R is the gas constant and T is the absolute temperature.

In earlier work, Horie *et al.*[37], who assumed that the two main epoxy–amine reactions, i.e. those involving primary and secondary amines, are autocatalytic and have the same reactivity, derived that the kinetics could be described by the relationship $d\alpha/dt = (k_1 + k_2\alpha)(1 - \alpha)(B - \alpha)$, where B is the initial ratio of amine to epoxide groups. It can be seen that if $B = 1$ (equal stoichiometry), the model of Horie *et al.*[37] becomes a special case of equation (4) where $m = 1$ and $n = 2$. However, the third type of reaction in an epoxy cure, i.e. the etherification reaction, was not taken into consideration in this model, and the observed deviation of the model at high levels of conversion was attributed (not entirely correctly) to gelation[14,37].

To obtain a first estimate of the reaction order n, equation (4) is modified to give the following:

$$\ln(d\alpha/dt) = \ln(k_1 + k_2\alpha^m) + n\ln(1 - \alpha) \quad (5)$$

Except for the initial region, a plot of $\ln(d\alpha/dt)$ *versus* $\ln(1 - \alpha)$ is expected to be linear with a slope n. Equation (4) can then be further rearranged to give:

$$\ln\{[(d\alpha/dt)/(1 - \alpha)^n] - k_1\} = \ln(k_2) + m\ln(\alpha) \quad (6)$$

The first term of equation (6) can be computed by using the previously estimated k_1 and n values. Linearity is expected if the left-hand term of equation (6) is plotted vs. $\ln(\alpha)$, yielding a straight line whose slope and intercept allow estimation of the reaction order, m, and the autocatalysed kinetic constant, k_2, respectively. By applying the described procedure, preliminary kinetic parameters can be obtained on the first trial. However, to obtain more precise values, an iterative procedure should

be utilized. Equation (4) can also be rearranged to give the following form:

$$\ln(d\alpha/dt) - \ln(k_1 + k_2\alpha^m) = n\ln(1-\alpha) \qquad (7)$$

With k_2, m, and n estimated from the stated procedures, the left-hand terms of equation (7) can be plotted vs. $\ln(1-\alpha)$, and a new value of the reaction order n can be obtained from the slope. This new value of n is checked with the one obtained earlier and the same iterative procedure can be repeated until convergence of the m and n values to within 1% deviation is achieved.

RESULTS AND DISCUSSION

Kinetic analysis of epoxy blends with poly(ether imide)

The neat epoxy resin and its blends with 10, 20, 30, 40, and 50 phr (based on 100 parts of the epoxy resin) of PEI were cured at three different isothermal temperatures, i.e. 177, 187, and 197°C, and kinetic analysis was performed using the above kinetic models. To avoid crowding the diagrams, only the rate curves for the neat epoxy resin and its three blends with 10, 30, and 50 phr of PEI were plotted. The results are shown in *Figures 1a–c* for the rate curves obtained at the three isothermal temperatures, 177, 187, and 197°C, respectively. These rate curves are distinctly autocatalytic in nature, with the maximum rate being seen to occur at times of 18, 15, and 10 min after the start of the reaction, respectively, for isothermal reaction temperatures of 177, 187, and 197°C. The results shown in these figures also demonstrate that the presence of PEI in the epoxy resin does not effect a change in the autocatalytic nature. However, the reaction rate of the epoxy is clearly enhanced by the presence of poly(ether imide) since the maximum rate increases with the PEI content in the epoxy blends. The same effect on the epoxy reaction rate was also observed for all of the three temperatures studied.

The detailed individual values of ΔH and α_1 are shown in *Table 1*, which shows that the total heats of reaction ($\Delta H_{1o} + \Delta H_R$) were slightly influenced by the presence of PEI, with the value decreasing slightly with the PEI content in the epoxy blends. The average values are $\sim 550\,J\,g^{-1}$. Note that calculation of the heats of reaction for the blends was based on the net weight of the epoxy–amine resin in the blends with the weight of PEI in the epoxy blends being discounted. The decrease of ΔH with the increase in PEI should not be taken as a result of the PEI weight in the blend. Rather, this was an indication that the reaction mechanism was likely to be changed by the presence of PEI in the blends. A similar decrease in ΔH was also observed in neat epoxy resins cured with higher concentrations of amine curing agent. The table also shows that the ultimate conversions (α_1) are increased from about 82 to 94%, corresponding to the increase in cure temperature from 177 to 197°C, indicating that the reactions would reach diffusion control (vitrification) regions at progressively higher conversions when higher reaction temperatures are used.

These data for the epoxy and its blends with PEI were analysed using the proposed autocatalytic mechanism. The kinetic parameters were determined using the procedures explained earlier. Since there are two kinetic constants, k_1 and k_2, two activation energies, ΔE_1 and ΔE_2, could be obtained by plotting $\ln k_1$ and $\ln k_2$, respectively, *versus* $1/T$. *Figure 2* shows the plots of $\ln k_1$

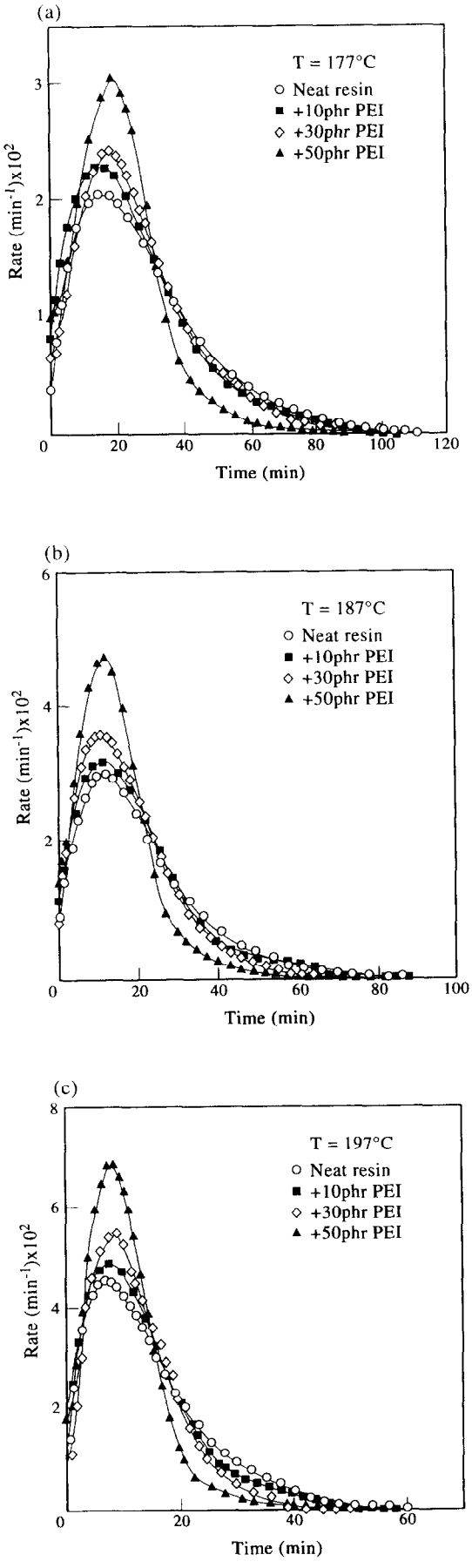

Figure 1 Plot of the reaction rate *versus* time for neat epoxy and 10, 30, and 50 phr PEI/epoxy blends at three different temperatures: (a) 177; (b) 187; (c) 197°C

Table 1 Heats of reaction of neat epoxy and blends of epoxy with various PEI contents

T (°C)	PEI in blends (phr)	ΔH_{Io} (J g^{-1})	ΔH_R (J g^{-1})	ΔH_T (J g^{-1})	α_1 (%)
177	0	444.8	101.1	546.0	81.5
177	10	468.5	87.1	555.6	84.3
177	20	448.1	87.8	535.9	83.6
177	30	426.8	89.8	516.6	82.6
177	50	419.9	92.6	512.5	81.9
187	0	482.2	76.4	558.6	86.3
187	10	484.5	58.9	543.4	89.2
187	20	493.2	51.0	544.2	90.6
187	30	476.4	55.9	532.3	89.5
187	50	467.6	52.5	520.1	89.9
197	0	550.7	41.9	592.6	92.9
197	10	543.7	27.6	571.3	95.2
197	20	553.3	28.7	582.0	95.1
197	30	529.1	30.8	559.9	94.5
197	50	507.6	40.6	548.2	92.6

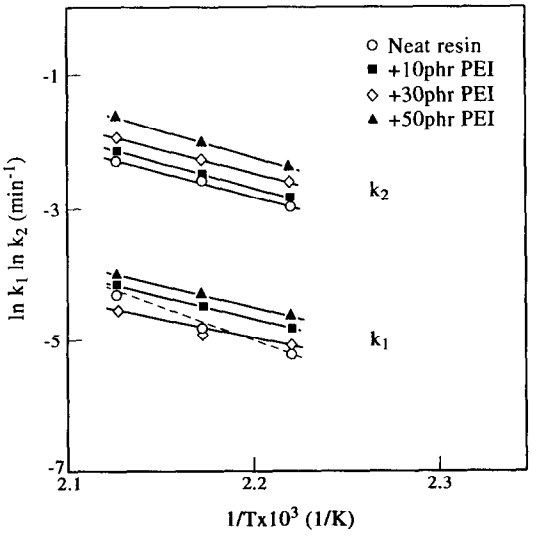

Figure 2 Plots of $\ln k_1$ and $\ln k_2$ against $1/T$ for neat resin and 10, 20, 30, and 50 phr PEI/epoxy blends in an autocatalysed reaction

or $\ln k_2$ vs. $1/T$, from which the activation energies were determined for the epoxy and its blends. The rate constants which were obtained through considerable iteration and graphic procedures are listed in *Table 2*. The reaction orders, m and n, are approximately 0.5 and 1.4, respectively, and the orders do not seem to vary much for the epoxy or the blends with different PEI contents. The values of ΔE_1 and ΔE_2 obtained in this study for the neat amine-cured TGDDM epoxy were 80.2 and 60.9 kJ mol^{-1}, respectively, which agreed well with those reported in the literature[31]. In comparison with this amine-cured tetrafunctional TGDDM epoxy, another common difunctional epoxy resin, the amine-cured diglycidyl ether of bisphenol-A (DGEBA) epoxy, has been reported to have a similar value of ΔE_1, but the value of ΔE_2 is lower (43–46 kJ mol^{-1})[14,30]. In comparison to the TGDDM epoxy, the amine-cured TGDDM–PEI blends exhibited lower activation energies (50–53 kJ mol^{-1}). The activation energy for k_2 of the epoxy blends remained much the same ($\Delta E_2 = 58$–61 kJ mol^{-1}) as that of the neat epoxy.

Table 2 Autocatalytic model constants for PEI-modified TGDDM epoxy blends

T (°C)	m	n	$k_1 \times 10^3$ (min^{-1})	$k_2 \times 10^3$ (min^{-1})	E_{a1} (kJ mol^{-1})	E_{a2} (kJ mol^{-1})	$\ln A_1$	$\ln A_2$
Neat epoxy								
177	0.60	1.47	3.49	48.7				
187	0.57	1.37	8.15	76.4	80.2	60.9	16.2	13.2
197	0.50	1.26	13.6	100.1				
Epoxy/PEI (10 phr)								
177	0.64	1.33	8.1	58.0				
187	0.55	1.47	11.0	81.9	53.8	58.6	11.7	13.0
197	0.48	1.23	15.6	116.1				
Epoxy/PEI (20 phr)								
177	0.66	1.38	6.95	64.3				
187	0.59	1.37	10.9	92.6	51.7	61.1	11.3	13.3
197	0.48	1.26	12.3	133.7				
Epoxy/PEI (30 phr)								
177	0.71	1.63	6.2	72.6				
187	0.53	1.50	7.5	100.5	50.6	59.6	11.0	13.3
197	0.65	1.44	10.6	142.9				
Epoxy/PEI (50 phr)								
177	0.65	1.30	9.6	95.2				
187	0.60	1.20	13.6	132.5	52.4	61.5	11.4	13.4
197	0.73	1.29	18.1	197.7				

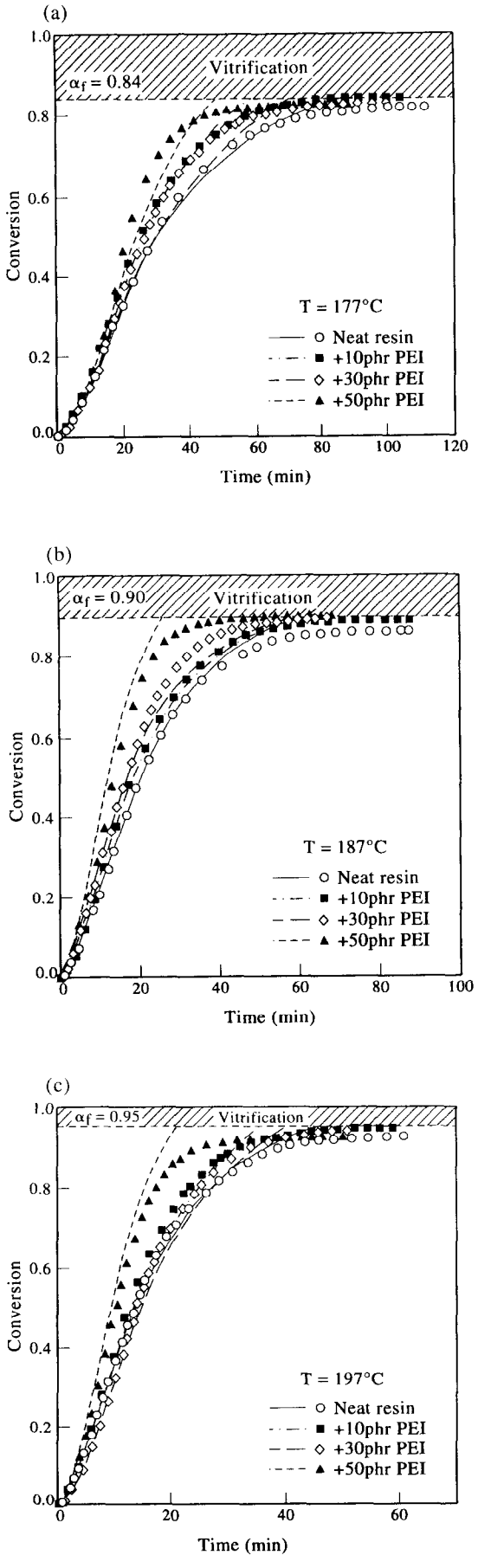

Figure 3 Comparison between the autocatalytic model and data for neat epoxy and 10, 30, and 50 phr PEI/epoxy blends at three different temperatures: (a) 177; (b) 187; (c) 197°C

Table 3 Glass transition temperatures of epoxy and PEI phases of epoxy/PEI blends in uncured or fully cured states

PEI content in blends (phr)	T_g of uncured blend (°C)	T_g of fully cured blend (°C)	
		PEI phase	Epoxy phase
0	3.3[a]	None	223.3
10	5.5	189.6	219.4
20	6.5	190.6	218.9
30	10.9	191.5	218.1
50	17.0	192.4	216.9

[a] T_g of uncured TGDDM = −12.0°C; T_g of DDS = 42.2°C

Apparently, the fact that ΔE_2 for the TGDDM blends is lower than the neat TGDDM epoxy indicates that the increase in the reaction rate might be associated with k_2. Since k_1 governs the early stage-autocatalytic reaction and k_2 affects the reaction after the initial autocatalytic stage, it could be expected that the rate increase might be more pronounced as the reaction proceeded beyond the initial stage.

The autocatalytic kinetic model and the rate constants obtained (listed in *Table 2*) were used to calculate empirical curves of conversions vs. time for the epoxy and its blends at all three isothermal cure temperatures. *Figures 3a–c* show that the empirical conversion curves fit the experimental data quite well until the cure reactions progress to the vitrification point. The model apparently describes the kinetics well, but diffusion control in the vitrified state limits the epoxy reactions from going any further. Vitrification is a state where the T_g of the reacting system exceeds the temperature of the system as a whole. The T_g of the epoxy phase of the blends was measured by d.s.c. immediately after the completion of isothermal cure. The T_g values of the cured epoxy blends were found to be 10–15°C above the cure temperatures of 177, 187, and 197°C, respectively. After vitrification any further progress in the cure reaction is virtually halted, and so, therefore, the extent of cure is limited[38]. This indicates that the cure kinetics in the later stage was indeed subjected to diffusion control as a result of vitrification.

Table 3 summarizes the T_g values of the neat epoxy and the PEI-rich and epoxy-rich phases of the epoxy–PEI blends after complete cure. As stated, vitrification imposes a limit on the epoxy conversion and therefore the T_g which is attainable at a specific cure temperature. Consequently, the T_g values of the neat epoxy after isothermal cure at different temperatures are ~10–15°C above the respective cure temperatures. The ultimate T_g of the neat epoxy at full cure (after heating to 300°C) was 223°C. The d.s.c. results showed clearly that the epoxy blends at full cure exhibit two T_g values, with one being for the PEI-rich phase and the other being for the epoxy-rich phase. The T_g values of the two major phases of the epoxy blends with various compositions are listed in *Table 3*, which shows a T_g for the PEI phase of 190°C and a T_g for the epoxy phase of 218°C. They are both clearly shifted when compared to the T_g values of the neat components (T_g = 210°C for neat PEI and 223°C for neat epoxy). This fact shows that phase segregation in the PEI–epoxy blends was incomplete. Entrapment of the PEI component in the epoxy domain, and vice versa, i.e. of the epoxy component in the PEI-rich phase, have both occurred. Our experimental results

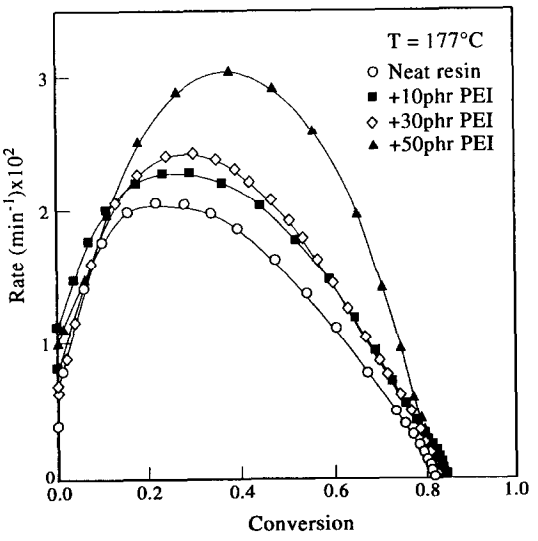

Figure 4 Plots of the reaction rate *versus* conversion for neat epoxy and its blends with 10, 30, and 50 phr of PEI, at 177°C

indicated that during mixing, the epoxy resin could be more easily dissolved in the PEI phase than could the DDS. Consequently, entrapment of further epoxy component, and less DDS, in the PEI-rich domain resulted in plasticization of the PEI domain after cure of the blends. The fact that there is a lower T_g for the PEI phase in the epoxy blends clearly supports such an argument. Due to uneven segregation or distribution of DDS in these two phases, a higher concentration of DDS was accumulated in the epoxy-rich domain. This phenomenon resulted in DDS being present in excess of the original 35 phr, thus causing a faster curing rate and a lower ultimate T_g of the epoxy phase in the blends.

Comparison between the neat epoxy and blends

Figure 4 shows the rate *versus* conversion curves for the epoxy resin and its blends with PEI of three different compositions (10, 30, and 50 phr) at a temperature of 177°C. This figure shows that the cure reaction rates are about the same for the epoxy and all of the epoxy/PEI blends at low levels of conversion. However, at higher conversions the reaction of the epoxy–PEI blends might progress at a higher rate than the neat epoxy resin. The cure rate vs. conversion at the other two cure temperatures (187 and 197°C) for the epoxy blends also demonstrated similar trends. Obviously, the higher conversions above which the cure rates show a difference coincide with the onset of the gel point, at which the gelled epoxy network starts to retard the progress of the cure reaction. By comparison, in the epoxy–PEI blends the crosslinked epoxy network is plasticized by the linear PEI polymer molecules. Once the cure reaction reaches the gel point, the reacting species in the neat epoxy would have less molecular mobility than those in the epoxy–PEI blends. As a result, the retardation effect on the epoxy cure of the epoxy–PEI blends was relatively less severe. This was expected to aid the reaction progress of the etherification, or even the secondary amine reaction, which occurred in the later stages of cure when the conversion had gone beyond the gel point.

Morphology evolution of epoxy–PEI blends during cure

Although the epoxy–PEI mixtures after blending were visually transparent and seemed homogeneous, T_g measurements using d.s.c. showed that the poly(ether imide) formed a separate phase, exhibiting only partial miscibility with the epoxy in the epoxy–PEI blends of all compositions before cure. Phase separation remained throughout the cure process; however, the phase domains and the dimensions underwent significant changes as the cure progressed. The phase morphology of the blend samples of three different compositions (10, 30, and 50 phr) was monitored by scanning electron microscopy (SEM) as a function of the time of cure when conducted at a temperature of 177°C. Morphology development of the blends at the other temperatures (187 and 197°C) was found to be similar. *Figure 5* shows scanning electron micrographs of the epoxy/PEI (10 phr) blend samples which had been cured for 5, 25, and 120 min of cure time at 177°C. *Figure 5a* shows that, initially, the PEI-rich-phase domain was relatively large (10–20 μm) and was distinctly separated from the surrounding epoxy-rich domain after 5 min of cure time. *Figure 5b* shows that after 25 min of cure time, the PEI-rich-phase domain was then gradually starting to be broken up into smaller particulate discrete domains, which were finely separated further by the reacting/crosslinking epoxy component originally dissolved in the PEI-rich domain. The micrograph shown in *Figure 5d* shows that at the end of cure (120 min), the PEI-rich domain clearly exists as fine dispersed particles (<1 μm), surrounded by the only continuous epoxy-phase domain.

Figure 6 shows scanning electron micrographs of the epoxy/PEI (30 phr) blend after 10, 15, 22, and 120 min of cure time, at a temperature of 177°C. The micrograph in *Figure 6a* shows that initially the PEI-rich and epoxy-rich domains were interdispersed, with no clear phase boundaries, after 10 min of cure time. Gradually, after 15 min of cure time, when the blend was approaching a gel state, two distinct regions (a fluffy, brighter region, and a smooth, darker region) appeared, as shown in *Figure 6b*. The fluffy, brighter region was a PEI-rich-phase domain, in which nearly spherical epoxy particles of 1 μm or less were dispersed and surrounded by the continuous PEI domain. The epoxy particles apparently formed in the PEI-rich domain early in the cure stage (15 min), while the epoxy-rich domain was still relatively homogeneous. The darker region was an epoxy-rich phase, which still appeared quite homogeneous with no discernible dispersed particles or foreign domains. This fact indicates that the cure kinetics of the epoxy component dissolved in the PEI-rich domain progressed at a faster rate than did the epoxy component in the bulk epoxy-rich domain. *Figure 6c* (22 min of cure time) shows that as the crosslinking density continuously increases with cure duration, the particulate PEI domain was gradually precipitated in the epoxy-rich domain. At the end of cure (*Figure 6d*, after 120 min), bicontinuous PEI and epoxy domains were clearly observed in the cured blend, where the PEI-rich continuous domain contained fine spherical shaped epoxy particles (1–2 μm) and the epoxy-rich continuous domain contained easily identified PEI particulate precipitation.

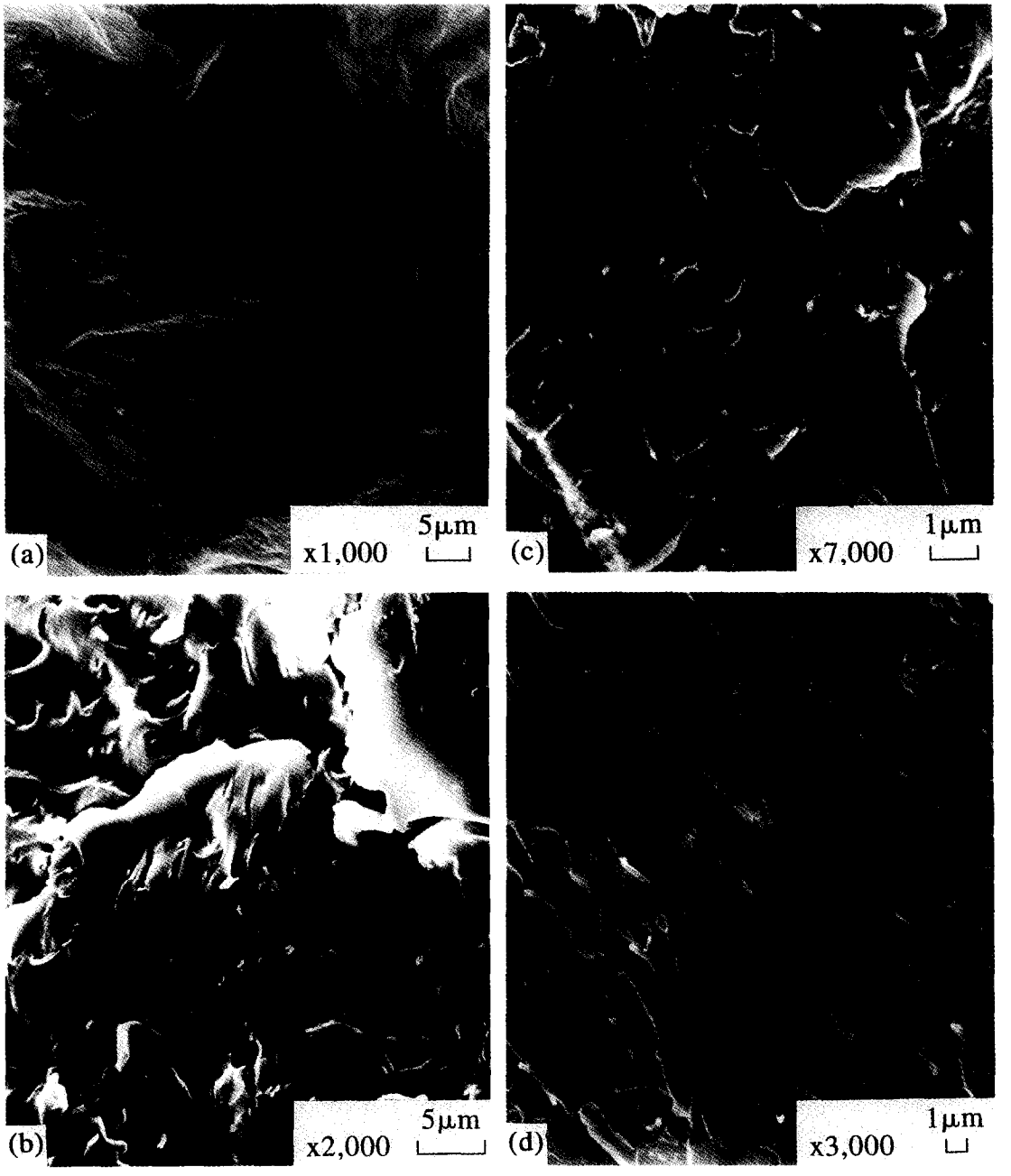

Figure 5 Scanning electron micrographs of 10 phr PEI/epoxy blend samples cured for different times at 177°C: (a) $t = 5$ min, $\alpha_I = 6.1\%$; (b) $t = 25$ min, $\alpha_I = 29.8\%$; (c) $t = 34$ min, $\alpha_I = 46.3\%$; (d) $t = 120$ min, $\alpha_I = 84.3\%$

Figure 7 shows scanning electron micrographs of epoxy/PEI (50 phr) blend samples that had been cured for 5, 23, 36, and 120 min of time, at a temperature of 177°C. *Figure 7a* shows that, initially, after ~5 min of reaction at 177°C, the fractured surface displayed two grossly separated domains, i.e. the PEI-rich phase and the epoxy-rich domains, as distinct regions (the fluffy, brighter region, and the smooth, darker region, respectively). However, it was still difficult to distinguish discontinuous from continuous domains. The micrograph shown in *Figure 7b* (blend sample after 23 min of cure time) illustrates that as the cure progressed, the PEI and epoxy domains changed into a morphology of interpenetrating meshes, in which the PEI-rich domain resembled randomly coiled shavings and the epoxy-rich domain resembled branching coral skeletons. *Figure 7c* shows that as the cure continued to 36 min, the PEI-rich domain was clearly mesh-like and interconnecting, and thus continuous, while the coral-like epoxy domain was also interconnecting, and thus this was also continuous. *Figure 7d* shows that this morphology remained unchanged throughout the cure until the end of the curing process (120 min), by which time the morphology was completely fixed. The epoxy–PEI (50 phr) blend was now comprised of two intertwined continuous PEI and epoxy domains. This morphology is different from that of the epoxy blends with lower PEI compositions, where as was discussed earlier, the two continuous phase domains, namely epoxy-rich and PEI-rich, are grossly separated. In addition, in these two domains the epoxy component is precipitated in the PEI-rich domain, and vice versa, the PEI component is precipitated in the

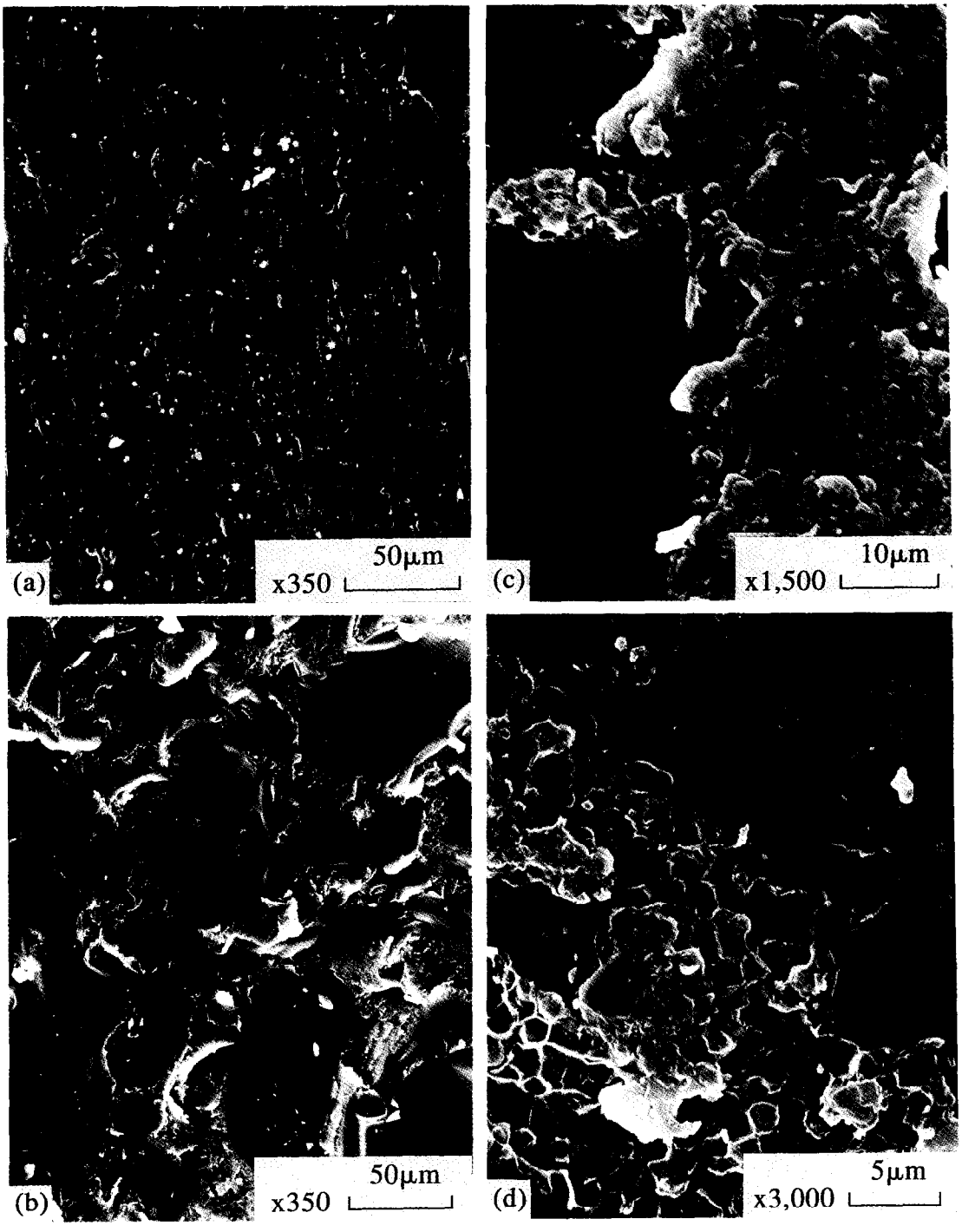

Figure 6 Scanning electron micrographs of 30 phr PEI/epoxy blend samples cured for different times at 177°C: (a) $t = 10$ min, $\alpha_I = 7.3\%$; (b) $t = 15$ min, $\alpha_I = 29.2\%$; (c) $t = 22$ min, $\alpha_I = 40.6\%$; (d) $t = 120$ min, $\alpha_I = 82.6\%$

epoxy-rich domain. In contrast, the two interpenetrating continuous domains of the epoxy–PEI (50 phr) blend were largely thermoplastic (PEI) and thermosetting (epoxy) in nature, with no apparent precipitation of one component in the other.

In order to provide a baseline comparison of the morphology evolution of the epoxy blends observed in this study and discussed as above, the fractured surface of the neat epoxy samples at various cure states were also examined by SEM. *Figure 8* shows scanning electron micrographs of neat epoxy samples that had been cured for 5, 18, 27, and 120 min, at a temperature of 177°C. The fracture surfaces all revealed a bland plane strain propagation, with no visible phase domains or boundaries.

To summarize, the morphology of the blends not only changed as a function of the cure time, but was also affected by the blend compositions. *Figure 9* shows a series of schematic diagrams of morphology development for the epoxy–PEI blends at different cure states, as well as different compositions, with the y-axis representing the blend composition, and the x-axis representing the time of cure. These schematic diagrams show that the morphology of the blends were all similar at low levels of

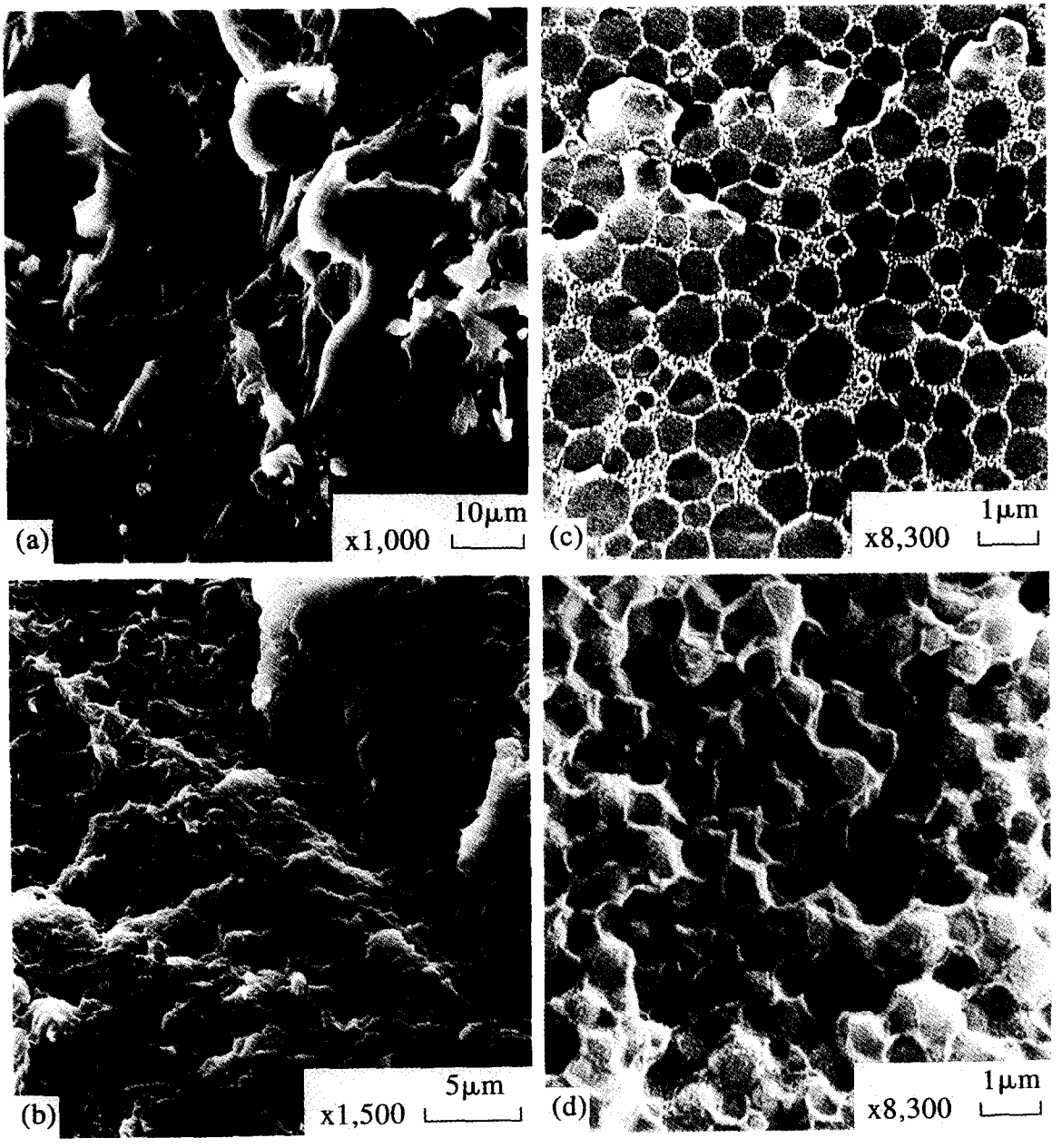

Figure 7 Scanning electron micrographs of 50 phr PEI/epoxy blend samples cured for different times at 177°C: (a) $t = 5$ min, $\alpha_I = 5.0\%$; (b) $t = 23$ min, $\alpha_I = 26.3\%$; (c) $t = 36$ min, $\alpha_I = 50.5\%$; (d) $t = 120$ min, $\alpha_I = 81.4\%$

conversion. As the cure time is increased, and thus the levels of conversion become higher, the epoxy blend with 10 phr of PEI or lower develops a morphology with the epoxy-rich phase forming the only continuous domain. The epoxy blends with 50 phr of PEI or higher, however, eventually develop a morphology of two continuous intertwined meshes, with one being the continuous epoxy domain and the other being the continuous PEI domain. For the blends with intermediate compositions, the fractured surface exhibits a mixed pattern of these two distinct morphologies. For example, the morphology of the epoxy blend with 30 phr of PEI displays an intermingled pattern, which contained a PEI-rich-continuous-phase domain resembling the morphology observed in the epoxy blends with low PEI contents, while another continuous domain shows interpenetrating PEI–epoxy meshes resembling the morphology of the epoxy blends with high PEI contents. Similar morphology changes corresponding to the thermoplastic contents have also been reported for other thermosetting/thermoplastic blend systems[39–42]. We have reported earlier interesting results in thermoplastic-modified bisphenol-E dicyanate resins, where the morphology and its correlation with properties was well described by a novel mechanical model[42].

CONCLUSIONS

An autocatalytic mechanism was observed for amine-cured epoxy–poly(ether imide) blends over a range of compositions. Kinetic parameters for the epoxy blends were obtained and the proposed kinetic model was found to describe well the cure behaviour of the epoxy and its blends up to the vitrification point. Although the reaction mechanism of the epoxy blends remained the same as that of the neat epoxy, the reaction rates of

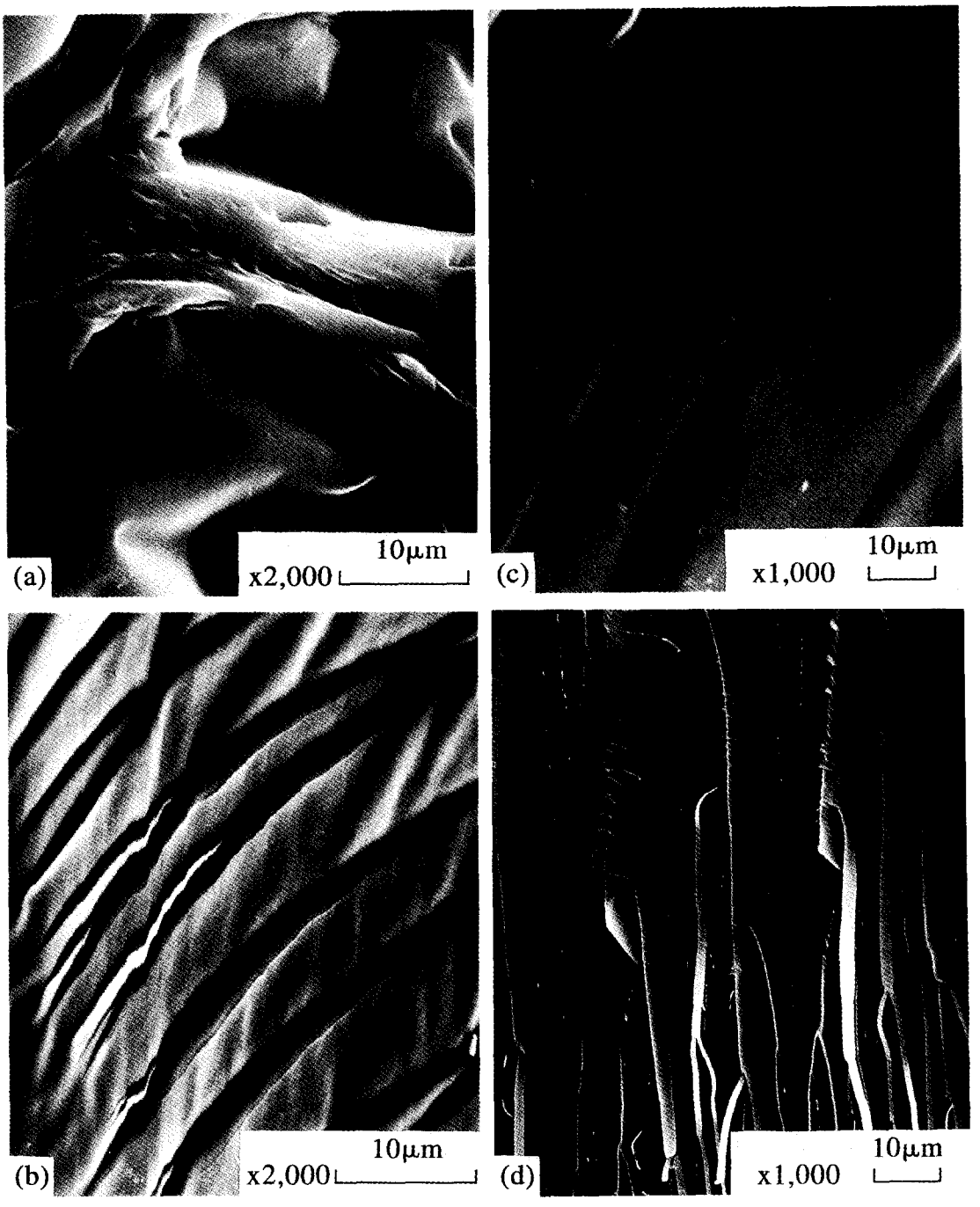

Figure 8 Scanning electron micrographs of neat epoxy samples cured for different times at 177°C: (a) $t = 5$ min, $\alpha_I = 4.6\%$; (b) $t = 18$ min, $\alpha_I = 24.7\%$; (c) $t = 27$ min, $\alpha_I = 42.9\%$; (d) $t = 120$ min, $\alpha_I = 81.5\%$

the blends were found to be higher than the latter. The initial reaction rates were found to be comparable for the neat epoxy and the epoxy–PEI blends for all compositions; however, as the cure progressed to the gel state, where effects of diffusion of the reacting species became a controlling factor, the epoxy–PEI blends exhibited a higher reaction rate.

To probe the mechanism of the observed difference in the cure kinetics between the epoxy–PEI blends and the neat epoxy, the morphology development of the blends, as the cure progressed from the initial to the final stages, was examined using SEM. For the epoxy–PEI blends, as the cure progressed, the phase domains went through a series of changes. At low extents of cure, partial miscibility existed between the epoxy and PEI phases, and the domain boundary was less obvious. As the cure progressed, segregation of the phases became more apparent, and the domains changed in relative sizes. As a result, the amine curing agent (DDS) was unevenly distributed, and local segregation of DDS in the epoxy-rich domain owing to phase separation resulted in a slightly higher concentration of DDS. In addition, the epoxy network could be plasticized by the linear PEI polymer chains. Both of these factors resulted in a higher reaction rate for the epoxy–PEI blends. The morphology of the final cured epoxy blends was consistently reproducible and was found to be dependent on the content of PEI in the blends. The

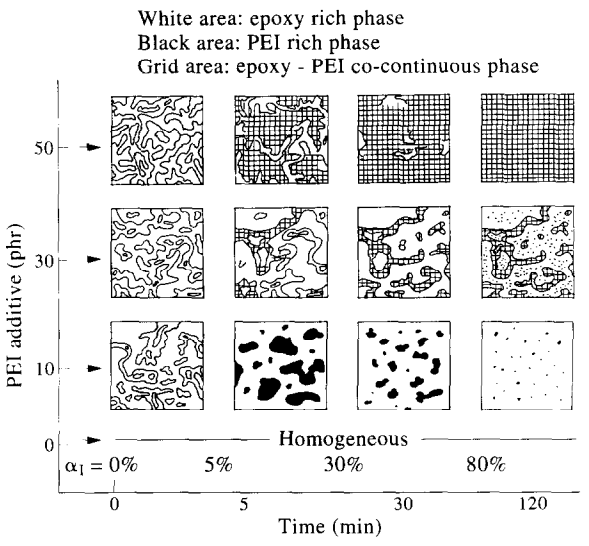

Figure 9 Schematic representation of the morphology of PEI/epoxy blends at various cure states and blend compositions

morphology of the epoxy blends changed from a continuous epoxy/discrete PEI pattern at low PEI contents (10 phr or lower) to an intertwined continuous PEI/epoxy strand pattern at a PEI content of 40 phr, or higher. These phase-separated morphological structures have been found to be common in many thermoplastic-modified thermosetting resins.

ACKNOWLEDGEMENTS

The authors acknowledge financial support (NSC 83-0405-E006-064) provided by the National Science Council of the Republic of China. The instrument support of scanning electron microscopy, provided by the Analytical Instrument Center (Tainan, Taiwan) of the National Science Council, is also appreciated.

REFERENCES

1 Kinloch, A. J., Shaw, S. J., Tod, D. A. and Hunston, D. L. *Polymer* 1983, **24**, 1341
2 Kunz, S. C., Sayre, J. A. and Assink, R. A. *Polymer* 1982, **23**, 1897
3 Pearson, R. A. and Yee, A. F. *J. Mater. Sci.* 1986, **21**, 2475
4 Bucknall, C. B. and Partridge, I. K. *Polymer* 1983, **24**, 639
5 Bucknall, C. B., Gomez, C. M. and Quintard, I. *Polymer* 1994, **35**, 353
6 Bucknall, C. B. and Gilbert, A. H. *Polymer* 1989, **30**, 213
7 Hourston, D. J. and Lane, J. M. *Polymer* 1992, **33**, 1379
8 di Liello, V., Martuselli, E., Musto, P., Rogosta, G. and Scarrinzi, G. *J. Polym. Sci. Polym. Phys. Edn* 1994, **32**, 409
9 Chen, M. C., Hourston, D. J. and Sun, W. B. *Eur. Polym. J.* 1992, **28**, 1471
10 Ohsako, T., Nagura, K. and Nozue, I. *Polymer* 1993, **34**, 5080
11 Pearson, R. A. and Yee, A. F. *Polymer* 1993, **34**, 3658
12 Woo, E.M., Bravenec, L. D. and Seferis, J. C. *Polym. Eng. Sci.* 1994, **34**, 1664
13 Hedrick, J. C., Patel, N. M. and McGrath, J. E. *ACS Adv. Chem. Ser.* 1993, **233**, 293
14 Sourour, S. and Kamal, M. R. *Thermochim. Acta* 1976, **14**, 41
15 Sung, C. S. P., Pyun, E. and Sun, H. L. *Macromolecules* 1986, **19**, 2922
16 Matejka, L. and Dusek, K. *Macromolecules* 1989, **22**, 2902
17 Matejka, L. and Dusek, K. *Macromolecules* 1989, **22**, 2911
18 Mijovic, J., Fishbain, A. and Wijana, J. *Macromolecules* 1992, **25**, 979
19 Mijovic, J., Fishbain, A. and Wijana, J. *Macromolecules* 1992, **25**, 986
20 Mijovic, J. and Wijaya, J. *Polymer* 1994, **35**, 2683
21 Buckley, L. and Roylance, D. *Polym. Eng. Sci.* 1982, **22**, 166
22 Johncock, P., Porecha, L. and Tudgey, G.F. *J. Polym. Sci. Polym. Chem. Edn* 1985, **23**, 291
23 Duffy, J. V., Hui, E. and Hartmann, B. *J. Appl. Polym. Sci.* 1987, **33**, 2959
24 Buist, G. J., Hagger, A. J., Jones, J. R., Barton, J. M. and Wright, W. *Polymer* 1988, **29**, 5
25 Min, B.-G., Starchurski, Z. H. and Hodgkin, J. H. *Polymer* 1993, **34**, 4488
26 St. John, N. A. and George, G. A. *Polymer* 1992, **33**, 2679
27 Woo, E. M. and Seferis, J. C. *J. Appl. Polym. Sci.* 1990, **40**, 1237
28 Nam, J.-D. and Seferis, J. C. *J. Appl. Polym. Sci.* 1993, **50**, 1555
29 Prime, R. B. in 'Thermal Characterization of Polymeric Materials' (Ed. E. A. Turi), Academic, New York, 1981, Ch. 5, p. 435
30 Barton, J. M. *Polymer* 1980, **21**, 603
31 Mijovic, M. R. *Polym. Eng. Sci.* 1974, **14**, 231
32 Kenny, J. M. *J. Appl. Polym. Sci.* 1994, **51**, 761
33 Ryan, M. E. and Dutta, A. *Polymer* 1979, **20**, 203
34 Cole, K. C. *Macromolecules* 1991, **24**, 3093
35 Cole, K. C., Hechler, J.-J. and Noel, D. *Macromolecules* 1991, **24**, 3098
36 Chiao, L. *Macromolecules* 1990, **23**, 1286
37 Horie, K., Hiura, H., Sawada, M., Mida, I. and Kambe, H. *J. Polym. Sci. (Part A1)* 1970, **8**, 1357
38 Enns, B. J. and Gillham, J. K. *ACS Adv. Chem. Ser.* 1983, **203**, 27
39 George, G. A., Clarke, P. C., St. John, N. A. and Friend, G. *J. Appl. Polym. Sci.* 1991, **42**, 643
40 Woo, E. M., Shimp, D. A. and Seferis, J. C. *Polymer* 1994, **35**, 1658
41 Yamanake, K., Takagi, Y. and Inoue, T. *Polymer* 1989, **60**, 1839
42 Woo, E. M., Su, C. C., Kuo, J.-F. and Seferis, J. C. *Macromolecules* 1994, **27**, 5291